Author Manuscript

Author Manuscript

Author Manuscript

Author Manuscript

HHS Public Access

Author manuscript

Neuroimage. Author manuscript; available in PMC 2016 November 14.

Published in final edited form as:

Neuroimage. 2016 October 15; 140: 33–40. doi:10.1016/j.neuroimage.2015.09.068.

Simultaneous transcranial direct current stimulation (tDCS) and whole-head magnetoencephalography (MEG): assessing the impact of tDCS on slow cortical magnetic fields

Eliana Garcia-Cossio[a,b,c], **Matthias Witkowski**[a,b], **Stephen E. Robinson**[d], **Leonardo G. Cohen**[e], **Niels Birbaumer**[a,f], and **Surjo R. Soekadar**[a,b,*]

[a] Institute of Medical Psychology and Behavioral Neurobiology and MEG Center, University of Tübingen, 72076 Tübingen, Germany [b] Applied Neurotechnology Lab, Department of Psychiatry and Psychotherapy, University of Tübingen, 72076 Tübingen, Germany [c] Donders Centre for Brain, Cognition and Behavior, Department of Artificial Intelligence, Radboud University Nijmegen, Nijmegen, The Netherlands [d] MEG Core Facility, National Institute of Mental Health (NIMH), NIH, Bethesda, MD 20892, USA [e] Human Cortical Physiology and Stroke Neurorehabilitation Section, National Institute of Neurological Disorders and Stroke (NINDS), NIH, Bethesda, MD 20892, USA [f] Ospedale San Camillo, Istituto di Ricovero e Cura a Carattere Scientifico, 30126 Venezia, Italy

Abstract

Transcranial direct current stimulation (tDCS) can influence cognitive, affective or motor brain functions. Whereas previous imaging studies demonstrated widespread tDCS effects on brain metabolism, direct impact of tDCS on electric or magnetic source activity in task-related brain areas could not be confirmed due to the difficulty to record such activity simultaneously during tDCS. The aim of this proof-of-principal study was to demonstrate the feasibility of whole-head source localization and reconstruction of neuromagnetic brain activity during tDCS and to confirm the direct effect of tDCS on ongoing neuromagnetic activity in task-related brain areas. Here we show for the first time that tDCS has an immediate impact on slow cortical magnetic fields (SCF, 0–4 Hz) of task-related areas that are identical with brain regions previously described in metabolic neuroimaging studies. 14 healthy volunteers performed a choice reaction time (RT) task while whole-head magnetoencephalography (MEG) was recorded. Task-related source-activity of SCFs was calculated using synthetic aperture magnetometry (SAM) in absence of stimulation and while anodal, cathodal or sham tDCS was delivered over the right primary motor cortex (M1). Source reconstruction revealed task-related SCF modulations in brain regions that precisely matched prior metabolic neuroimaging studies. Anodal and cathodal tDCS had a polarity-dependent impact on RT and SCF in primary sensorimotor and medial centro-parietal cortices. Combining tDCS and whole-head MEG is a powerful approach to investigate the direct effects of

* Corresponding author at: University of Tübingen, Calwerstr. 14, 72076 Tübingen, Germany. Fax: +49 7071 2982625. surjo.soekadar@uni-tuebingen.de (S.R. Soekadar).

Appendix A. Supplementary data

Supplementary data to this article can be found online at http://dx.doi.org/10.1016/j.neuroimage.2015.09.068.

Author Manuscript Author Manuscript Author Manuscript Author Manuscript

transcranial electric currents on ongoing neuromagnetic source activity, brain function and behavior.

Keywords

Transcranial direct current stimulation; Magnetoencephalography; Slow cortical fields; Source-reconstruction

Introduction

Sensory, motor and cognitive brain functions are causally linked to electrochemical processes reflected in large-scale cortical activity that can be recorded as oscillatory (Kayser et al., 2009; Wang, 2010) or evoked electrical or magnetic brain activity (Birbaumer et al., 1990). Previous work has demonstrated that transcranial direct current stimulation (tDCS), the application of weak electric DC currents of 1–2 mA through contact electrodes placed over the scalp, can modulate cortical excitability in a polarity specific way, and affect cognition (Monti et al., 2013; Nitsche et al., 2012; Santarnecchi et al., 2013), visuo-motor learning (Antal et al., 2004) or motor performance (Hendy and Kidgell, 2014; Hummel et al., 2005). The underlying neurophysiological mechanisms mediating these effects, however, are not understood (Dayan et al., 2013), partly because of the difficulty to record neural activity at high temporal and spatial resolution while transcranial electric currents are applied. The main difficulty is to eliminate electromagnetic artifacts that by many orders of magnitude exceed the brain's endogenous electric or magnetic activity.

Only recently, new strategies, e.g. Transcranial Electric Stimulation during Assessment of Neuromagnetic Activity (TESANA) (Soekadar et al., 2013a), have been developed that overcome this limitation (Soekadar et al., 2013a, 2014). While successful combination of transcranial electric stimulation (tES) with electroencephalography (EEG) was demonstrated across various studies (Helfrich et al., 2014; Soekadar et al., 2014; Voss et al., 2014), spatial resolution of EEG is limited and assessment of brain oscillatory activity immediately underneath stimulation electrodes is not possible in such experimental setup (Soekadar et al., 2014). Thus, there is currently no study available that assessed the direct impact of tDCS on neuromagnetic brain activity in task-related brain areas including cortical areas in the immediate proximity and underneath the stimulation electrodes, an issue investigated in this proof-of-principal study.

A better understanding of the direct effects of tDCS on neuromagnetic brain activity will not only provide critical information on possible mechanisms underlying tDCS effects, but also provide new insights into the relationship between brain physiology and behavior. Ultimately, this may lead to the refinement of existing and development of new stimulation protocols used e.g. in the treatment of various neuropsychiatric disorders, e.g. depression, stroke or chronic pain (Kuo et al., 2014).

The underlying key-mechanisms of tDCS effects were thought to relate to stimulated neural cells' resting membrane potential that become either de- or hyperpolarized depending on their orientation relative to the electrical field (Creutzfeld et al., 1962; Purpura and

Author Manuscript Author Manuscript Author Manuscript Author Manuscript

McMurtry, 1965). As modulation of cortical excitability as measured by e.g. motor evoked potentials (MEP) sustained after the electric current was switched off (Nitsche and Paulus, 2000), other mechanisms such as synaptic plasticity involving early gene expression and protein synthesis previously shown in animal studies (Gartside, 1968) influencing long-term depression (LTD) and potentiation (LTP) (Feldman, 2009) were postulated (Paulus, in review). However, the exact mechanisms underlying the effects of tDCS are still incompletely understood, particularly how neurophysiological effects link to brain function and human behavior.

Based on previous studies that showed consistent short-term and long-lasting effects of tDCS on motor learning and performance (Boggio et al., 2006; Hummel et al., 2005) as well as motor cortical excitability (Nitsche and Paulus, 2000) and regulation of sensorimotor rhythms (SMR) (Soekadar et al., 2015), we have chosen the motor domain for our investigation.

The most consistent relationship between cortical excitability and electric brain activity was found for slow cortical potentials (SCP) (Rockstroh et al., 1989) and their magnetic counterpart, the slow cortical fields (SCF). SCPs (mainly <1 Hz, but can extent to up to ~4 Hz; Rösler et al., 1997; Birbaumer et al., 1990) mainly reflect synaptic activity of superficial apical dendrites that are modulated in their activity by non-specific thalamic inputs, long-range intercortical and cortico-cortical connections. It was shown that a negative deflection of SCPs is associated with increased cortical excitability that goes along with increased multi-unit activity (Rebert, 1973), increased high-frequency field potentials (Pellicciari et al., 2013) and higher amplitude of evoked potentials, e.g. P300 (Ergenoglu et al., 1998). Importantly, SCP negativity correlates with improved behavioral performance (Birbaumer et al., 1990). This suggests that tDCS-dependent behavioral effects might be mediated by modulation of SCPs and SCFs, respectively. We thus strived to assess whether tDCS has an immediate effect on motor task-related SCF and if the case, how different stimulation polarities applied over the primary motor cortex (M1) would influence SCFs across various task-related brain regions.

Such knowledge would complement and extend previous studies that investigated metabolic signal changes during tDCS, e.g. during finger tapping (Antal et al., 2011; Lang et al., 2005) or a reaction time task (Stagg et al., 2009). These studies provided detailed topographic information on cortical and sub-cortical task-related brain activations. For instance, a neuroimaging study that used positron emission tomography (PET) of regional cerebral blood flow (rCBF) during finger tapping while anodal or cathodal tDCS was applied over the left primary motor cortex (M1) showed bilateral increase in rCBF in a widespread task-related network that comprised the sensorimotor cortex and posterior parietal cortex (PPC) on both hemispheres (Lang et al., 2005). The PPC, particularly Brodmann area 7 comprising the precuneus and superior parietal lobule (SPL), was shown to relate to visuo-motor integration, e.g. in reaching and grasping (Konen et al., 2013), but also performance in reaction-time tasks (Hinds et al., 2013). Other studies using functional magnetic resonance imaging (fMRI) found blood-oxygenation level dependent (BOLD) signal changes in similar brain regions. While anodal tDCS increased activation of M1 and the supplementary motor area (SMA) on the stimulated hemisphere, cathodal tDCS resulted in an increased activation

Author Manuscript Author Manuscript Author Manuscript Author Manuscript

of the contralateral M1 and dorsal premotor cortex (PMd) (Antal et al., 2011). While these studies provided important information on global effects of tDCS on brain metabolism and their spatial distribution, they could not provide information on the underlying neuronal activity as investigated here. Thus, the direct impact of tDCS on whole-head neuromagnetic activity could not be confirmed yet.

As the temporal scale of BOLD signal changes (<0.5 Hz) overlap with cortical steady potentials and both signals show correlative changes suggesting shared underlying neural substrates and neuronal dynamics (Hiltunen et al., 2014), this direct relationship between BOLD fMRI and (infraslow) cortical steady potentials makes motor-related SCP an ideal candidate for this proof-of-principal study as localizations of task-related slow cortical fields (SCFs, the magnetic analogue of SCPs) and their magnitude recorded in absence and during tDCS can be compared with activation maps and tDCS-dependent modulations of metabolic signals described in previous fMRI studies. Additionally, it allows investigating how the impact of tDCS on SCFs relates to BOLD fMRI effects found in previous studies. One of the best-established experimental paradigms to study motor-related SCPs is the so called S1–S2 or go/no-go paradigm in which participants are instructed to press or withhold from pressing a button upon a visual cue (Birbaumer et al., 1990; Walter et al., 1964). While a first visual stimulus (S1) indicates to prepare for a motor action (button press), a second visual stimulus (S2) indicates what specific action should be performed, e.g. left, right or no button press. The resulting cortical electric fluctuation during and after presentation of S1 and S2 is called the contingent negative variation (CNV) in EEG or contingent magnetic variation (CMV) in MEG recordings (Elbert et al., 1994). Here we recorded the CMV and tested, after ensuring conformity of identified task-related brain regions with previous neuroimaging studies, whether reconstruction of SCF in task-related brain regions during simultaneous anodal or cathodal tDCS is possible and whether these reflect polarity-dependent impact of tDCS on motor task-performance.

Materials and methods

Participants

14 healthy volunteers (five female, all right handed, mean age 28.7 ± 3.2) without a history of neurological or psychiatric disorders were recruited at the University of Tübingen, Germany, and participated in this study. Prior to the first MEG session, location of the primary motor cortex (M1) was assessed by single pulse transcranial magnetic stimulation (TMS) according to Rossini et al. (1994). Three fiducial localization coils were placed at the nasion as well as the left and right pre-auricular area to allow recording of the participant's head position during MEG recordings. Coil positions of the recorded MEG data were co-registered with the structural magnetic resonance (MR) images offline. The study was approved by the Ethics Committee of the Medical Faculty at the University of Tübingen. All participants provided written informed consent before entering the study.

Magnetoencephalographic (MEG) recordings

Biomagnetic signals were recorded at a 586 Hz sampling rate with a bandwidth of 0–150 Hz while participants were seated upright in a whole-head 275-sensor MEG (CTF MEG® by

Author Manuscript Author Manuscript Author Manuscript Author Manuscript

MISL, Coquitlam, Canada) housed in a magnetically shielded room. Synthetic third gradient balancing was used to attenuate environmental magnetic interference.

Magnetic resonance imaging (MRI)

A cranial MRI exam in a 3-Tesla whole body scanner with a 12-channel head coil (Magnetom Trio®, Siemens, Erlangen, Germany) was performed in all participants. Vitamin E capsules served as markers for the nasion and preauricular areas corresponding to locations used for MEG head localization. To minimize movements, the participants' head was fixated during the MRI acquisition using two pieces of foam rubber. A T1-weighted structural scan of the whole brain was obtained using the sequence MPRAGE (matrix size = 256 × 256, 160 partitions, 1 mm^3 isotropic voxels, TA = 5:17 m, TR = 2300 ms, TE = 3.93 ms, flip angle = 8°, FOVRO = 256, FOVPE = 224, PAT = 2, PAT mode = GRAPPA) that served as anatomical reference.

Transcranial direct current stimulation (tDCS) in the MEG environment

Transcranial Electric Stimulation during Assessment of Neuromagnetic Activity (TESANA) was performed in accordance to Soekadar et al., 2013a. For tDCS, a direct current was applied to the participant's head using a commercial DC stimulator (DC Stimulator MR®, NeuroConn GmbH, Ilmenau, Germany, time resolution <1 ms, sample rate 2048 samples/s, max. 1% direct current fault tolerance). Two re-usable radio-translucent (non-ferromagnetic) rubber stimulator electrodes (size 70 × 40 mm, supplied by NeuroConn GmbH, Ilmenau, Germany) were placed over the right M1 (target electrode) and the left supra-orbital area (return electrode) (Fig. 1A) (Nitsche and Paulus, 2000). The battery-driven stimulator device was located outside the magnetically shielded room and delivered electric currents via a twisted pair of wires with a magnitude of 1 mA (current density: 0.038 mA/cm2). A conductive paste (Ten20®, D.O. Weaver, Aurora, CO, USA) was applied to the rubber electrodes to increase conduction between the scalp and the electrodes. Impedance levels were continuously assessed during stimulation and voltages were adapted accordingly. To avoid voltage to exceed 20 V, the maximum impedance level for automatic switch off was set to 20 kΩ and did not exceeded this threshold in any of the sessions.

Experimental design

Participants attended three experimental sessions over three different days and received either sham, anodal or cathodal stimulation in a pseudo-randomized order following a counterbalanced cross-over design. Each experimental session consisted of two blocks: a baseline block (in which the participants performed the task in absence of stimulation) and a stimulation block (in which different stimulation types, anodal, cathodal or sham stimulation, were applied during task performance) (Fig. 1C). Each block consisted of two runs with 65 trials.

During the stimulation block, tDCS was applied continuously after a ramp up phase of 30s. For sham stimulation, electric currents were switched off immediately after the ramp up phase, so that participants performed the task in absence of stimulation. No participant was able to differentiate between the different types of stimulation (see supplementary material, Supplementary Table S1).

Author Manuscript Author Manuscript Author Manuscript Author Manuscript

Participants were asked to press a button using their right or left index finger according to a cue presented on a display in front of them. To mask any transient auditory stimuli during the experiment, white noise was presented via two auditory tubes.

During the experiment, participants performed a classical go/no-go reaction time (RT) task consisting of a *warning* stimulus (S1) and an *imperative* stimulus (S2) (therefore also termed S1–S2 paradigm). During inter-trial-intervals (ITI), a white cross was shown in the middle of the screen indicating the participants to relax. The length of the ITIs was randomized between 4000 to 7000 ms (Fig. 1B). S1 was indicated by the word 'PREPARE' and shown in the center of the display for 200 ms. During the inter-stimulus interval (ISI) or preparation interval, a red cross was presented for 3200 ms followed by S2 shown for 200 ms. S2 was randomly chosen from three possible symbols: a red arrow to the right, a red arrow to the left or a red cross. Participants were instructed to press the left button as soon as they saw the arrow to the left, or the right button when they saw the arrow to the right. No button should be pressed when the red cross was shown. In total, 25 left and 25 right button press trials and 15 no-go trials were presented in each run. Each run lasted approximately 9 min. A short break of 3–4 min separated the two runs in each block. As participants received tDCS over their right M1, only physiological and behavioral data for contralateral left-button presses were analyzed.

Reaction time and accuracy assessment

Reaction times (RT) of left index finger button presses were calculated as the time between onset of S2 presentation and the actual button press (Boggio et al., 2006). RTs longer than 2 s and/or negative (when button-presses occurred before S2) were discarded. RT outliers were removed using an iterative implementation of the Grubbs Test (Grubbs, 1969), an established measure to detect outliers in a normally-distributed, univariate data set based on the difference between the mean of the sample and the most extreme data considering the standard deviation. RTs of each trial were normalized (ΔRT) to the mean RT of the baseline block. To test whether tDCS had polarity dependent effects on reaction times, a two-way repeated-measures ANOVA with ΔRT as dependent variable and 'stimulation type' (anodal, cathodal, sham) as between-subject factor and 'blocks' (baseline block, stimulation block) as within-subject factor was conducted. Post-hoc paired-samples Students t-tests were used when applicable and corrected for multiple comparisons (Bonferroni). Accuracy was calculated as percentage of correct button-press responses in each run. To examine whether tDCS had an effect on accuracy, a non-parametric two-way ANOVA with accuracy as dependent variable and 'stimulation type' (anodal, cathodal, sham) as between-subject factor and 'blocks' (baseline block, stimulation block) as within-subject factor was performed. Significance level for all statistical tests was set to $p \leq 0.05$.

MEG sensor space analysis

To verify conformity of the CMV's topographic distribution and time course with previous studies (Dammers and Ioannides, 2000; Elbert et al., 1994), a sensor space analysis of CMV recorded in absence of stimulation (during the baseline block) was performed in accordance to Elbert et al. (1994). For this purpose, MEG data was pre-processed using a Butterworth low-pass filter at 4 Hz ensuring inclusion of all CMV components (Walter et al., 1964).

Author Manuscript Author Manuscript Author Manuscript Author Manuscript

Muscle, cardiac and eye-movement related artifacts were removed using an independent component analysis (ICA). After pre-processing, the CMV grand average of blocks recorded in absence of stimulation was calculated across all participants. Analysis of MEG sensor data was performed using the open source toolbox Fieldtrip (Oostenveld et al., 2011) (http://run.nl/fcdonders/fieldtrip/).

Source localization and reconstruction of SCF in absence of stimulation

To identify brain regions showing task-related SCF modulations in absence of stimulation, MEG source analysis was performed using Synthetic Aperture Magnetometry (SAM) beamforming (Robinson and Vrba, 1999). This adaptive spatial filter was computed for each location on the individual brain using the entire array of MEG sensors. Estimates of source activity in each of the target locations were then obtained by projecting sensor signals through the corresponding spatial filter derived from a covariance matrix calculated over the entire time series. The estimates of source activity (virtual sensor signals) provide the same temporal resolution as the original MEG recordings (Hillebrand and Barnes, 2002). Source activity between 0–4 Hz was estimated at 5 mm^3 resolution throughout the whole brain. Before application of SAM beamforming, data was bandpass filtered from 0–4 Hz using a 3rd order infinite impulse response (IIR) filter. To avoid noise bias towards the center of the head (Robinson and Vrba, 1999), pseudo-z maps were calculated by dividing the estimated source power by the projected noise (Robinson and Vrba, 1999). Source power was calculated for two different time windows of interest: a baseline or *control window* from −1 to 0 s relative to S1 and an *active window* from −1 to 0 s relative to S2 (Rockstroh et al., 1989; Walter et al., 1964). Calculation of source power was performed for each run separately. In total, 2100 trials were included in the analysis (25 trials × 2 runs × 3 sessions × 14 participants).

For correct estimation and localization of MEG source activity relative to each participant's brain anatomy, the individual T1-weighted MR images were co-registered with the individual anatomical landmarks corresponding to the MEG fiducial markers and transformed to the head frame.

Statistical analysis of the source power images was performed using the open source software AFNI (http://afni.nimh.nih.gov/afni/). Source power (normalized by the projected noise) from the *control* and *active window* were contrasted across participants using a non-parametric paired-sample *t*-test (Wilcoxon). Individual source power maps of each window were non-linearly transformed into Talairach space before application of inter-individual statistics.

As SAM beamforming is based upon a current dipole model in which image solutions are proportional to the source magnitude and noise, the extent threshold for cluster level analysis was set as function of estimated source magnitude and sensor noise. Results were corrected for multiple comparisons using Monte Carlo simulations with significance levels set to $p \leq 0.05$ in combination with an extent threshold of 25 neighboring voxels.

Author Manuscript Author Manuscript Author Manuscript Author Manuscript

Source reconstruction of SCF time-course in task-related brain regions during tDCS

To demonstrate feasibility of source reconstruction in task-related brain regions immediately underneath the target electrode during active tDCS, SCF time courses of right M1 voxels that showed task-related SCF modulations in absence of stimulation were calculated.

Before estimation of the covariance matrix, signals were filtered from 0–30 Hz using a 6th order IIR filter. Reconstructed source signals were bandpass filtered between 0 and 4 Hz (using a 3rd order Butterworth filter), epoched over all trials from −5.5 to 2.5 s relative to S2, Hilbert transformed and then averaged.

Localization of stimulation dependent effects on SCF

Source localization and reconstruction of SCF during stimulation was performed in analogy to MEG source analysis performed for data recorded in absence of stimulation (see above). To localize the effects of tDCS on SCF, whole-brain (resolution 5 mm^3) source reconstruction of SCF (0–4 Hz) recorded during anodal and during cathodal stimulation was performed.

To calculate the stimulation dependent effect of tDCS on SCF, SCF source power during the *control window* was subtracted from SCF source power during the *active window*. Then, ΔSCFs were calculated for each stimulation type (anodal, cathodal or sham) by subtracting the SCF of the baseline block from the SCF of the stimulation block.

For the analysis of group data in a common anatomical space, anatomical data and SAM volumes were aligned into Talairach space using AFNI.

In order to detect polarity dependent tDCS effects on SCF, a non-parametric one-way ANOVA (Kruskal-Wallis) with ΔSCF as dependent variable and stimulation type (anodal, cathodal, sham) as independent variable was performed. Post-hoc non-parametric t-tests (Wilcoxon signed-rank test) were used to compare ΔSCF between stimulation types. Significance level of Monte Carlo simulations for multiple-comparison correction was set to $p \leq 0.05$ in combination with an extent threshold of 13 neighboring voxels.

Results

Reaction times and accuracy

A two-way ANOVA with the ΔRTs of the left hand as dependent variable revealed no significant main effect of ‘block’ ($F_{1,39} = 0.25$, $p = 0.62$) and ‘stimulation type’ ($F_{2,39} = 2.76$, $p = 0.076$), but a significant interaction ($F_{2,39} = 6.6$, $p \leq 0.01$).

Comparison of tDCS-effects across stimulation types using post-hoc t-tests showed that cathodal stimulation resulted in increased RTs (i.e. slower reaction) compared to sham ($p \leq 0.001$) and anodal stimulation ($p \leq 0.01$), while no difference in RT was found between anodal and sham stimulation ($p = 0.54$) (Fig. 2).

Additionally, the comparison of RTs between baseline and stimulation blocks using post-hoc t-tests revealed an increase under cathodal ($p \leq 0.01$), but no difference under sham ($p =$

Author Manuscript Author Manuscript Author Manuscript Author Manuscript

0.43) or anodal tDCS (p = 0.23). No session-to-session practice effect was found (see supplementary material, supplementary analysis and results).

Analysis of accuracies in absence of stimulation (baseline block) showed that participants reached 96.3 ± 9.0%, 95.4 ± 5.6% and 93.9 ± 13.4% correct button presses, and 97.6 ± 6.3%, 98.3 ± 3.5% and 93.3 ± 8.5% during the stimulation blocks (anodal, cathodal, sham).

Button presses were highly accurate across all participants, blocks (baseline block, stimulation block) and stimulation types (anodal, cathodal, sham). No statistical differences of button press accuracies were found between blocks or stimulation types ($\chi^2 = -0.1648$, p > 0.05).

MEG sensor space analysis

In agreement with prior literature (Dammers and Ioannides, 2000; Elbert et al., 1994), the topographic distribution and time course grand average of the CMV showed the typical event-related field activity over posterior centro-medial areas expected in a visuo-motor S1–S2 paradigm (Figs. 3A–B).

Source reconstruction of SCF and impact of tDCS

Source localization and reconstruction of task-related SCF in absence of stimulation showed SCF modulations in frontal, pre-motor, primary sensori-motor, posterior parietal and occipital brain regions accurately matching task-related brain regions described in previous metabolic neuroimaging studies (Antal et al., 2011; Lang et al., 2005; Stagg et al., 2009).

These regions particularly included the post-central cortices, precunei, as well as paracentral, posterior cingulate and inferior parietal lobules and cunei on both hemispheres (Fig. 3D). Task-related SCF modulations were also found in frontal areas that included the supplementary motor areas (SMA) and pre-central gyri of both hemispheres, as well as the left anterior cingulate and prefrontal cortex.

Time-course of SCF M1 during anodal and cathodal stimulation had the same characteristics as SCF M1 recorded in absence of stimulation (Fig. 3C) and resembled the typical CMV waveform (Fig. 3A) (Elbert et al., 1994).

A non-parametric one-way ANOVA with stimulation type (anodal, cathodal, sham) as independent variable and ΔSCF as dependent variable revealed a direct impact of tDCS on source localized SCF in the right (the primary stimulation site) and left pre-central gyrus and right and left PPC (precuneus) ($F = 6.20$, $p \leq 0.05$ corrected) (Figs. 4A–B). The right PPC included the right precuneus, right paracentral lobule and right posterior cingulate gyrus in which SCFs were weaker during anodal stimulation compared to sham ($p \leq 0.001$) (Fig. 4C), but not to cathodal stimulation (p = 0.09) or when comparing cathodal to sham stimulation (p = 0.17) (Fig. 4D). Furthermore, SCF in the left premotor cortex decreased under anodal tDCS compared to sham ($p \leq 0.05$) (Fig. 4C), but not under cathodal tDCS (p = 0.13) leaving this region unaffected (compared to sham stimulation (p = 0.73)) (Fig. 4D). Coordinates of SCF modulated by tDCS were located within task-related brain areas

Author Manuscript Author Manuscript Author Manuscript Author Manuscript

identified in absence of stimulation (for Talairach coordinates of all significant voxels please see supplementary materials, Supplementary Table S2).

On the other hand, field strength of SCF in the right pre-central gyrus (the primary stimulation site) increased during anodal tDCS compared to sham ($p \leq 0.01$) (Fig. 4C) and during cathodal compared to sham ($p \leq 0.05$) (Fig. 4D). Moreover, cathodal tDCS resulted in weaker SCFs in the non-stimulated left PPC compared to sham ($p \leq 0.05$) (Fig. 4D), but no difference was found in comparison to anodal stimulation ($p = 0.06$). Interestingly, anodal stimulation left this remote region in the sensory association cortex of the non-stimulated hemisphere unaffected (compared to sham, $p = 0.13$) (Fig. 4C).

Discussion

The aim of this proof-of-principal study was to demonstrate the feasibility of whole-head source localization and reconstruction of neuromagnetic brain activity during tDCS and to confirm the direct effect of tDCS on ongoing neuromagnetic activity in task-related brain areas. Whereas MEG characterization of brain activity below 1 Hz is particularly challenging due to interfering signals from environmental noise sources, a combination of noise-cancellation techniques, such as higher-order gradiometer formation and application of adaptive beamforming was applied in this study to improve reconstruction of slow cortical source activity.

Whole-head source localization and reconstruction of SCF during anodal and cathodal tDCS using TESANA was feasible and showed SCF modulations in brain areas that accurately matched those previously described in metabolic neuroimaging studies (Antal et al., 2011; Lang et al., 2005; Stagg et al., 2009). These brain areas comprised primary and higher order (association) cortical areas that are typically active in visuo-motor tasks involving high-level executive functions and action coordination (e.g. the medial and superior frontal gyri) (Floden and Stuss, 2006; Talati and Hirsch, 2005). Application of tDCS over the right M1 resulted in polarity-specific regulation of RT and magnitude of SCFs recorded from brain regions immediately underneath the stimulation electrode as well as task-related brain regions remote from the primary stimulation site. While anodal stimulation mainly influenced SCF on the stimulated hemisphere, cathodal stimulation in contrast affected SCF on the contralateral hemisphere (for Talairach coordinates see supplementary materials, Supplementary Table S2). This finding suggests the involvement of other mechanisms than de- or hyperpolarization of resting membrane potentials in areas directly exposed to the electrical field, e.g. short-term synaptic structural and functional remodeling. Although we found that tDCS-dependent SCF modulations were localized in task-related areas characterized in absence of stimulation (Fig. 3, Supplementary Table S2), source localization at higher spatial resolution than applied here might provide further evidence for the involvement of such mechanisms. As the return electrode placed over the contralateral supraorbital region is neither inert nor inactive, direct contribution of this electrode to the observed physiological effects cannot be excluded (Brunoni et al., 2012). Provided same polarity, the supraorbital return electrode may have influenced brain activity similar to the contralateral more posterior placement. In this context, it is particularly noteworthy that increased SCF in PPC changed in concert with the location of the anode, irrespective of the

Author Manuscript Author Manuscript Author Manuscript Author Manuscript

use as target or return electrode. This finding may point to a polarity- and hemisphere-specific effect of anodal tDCS on task-related areas that interferes with lateralized activity important for normal motor function possibly mediated via fronto-parietal networks (Keeser et al., 2011; Pena-Gomez et al., 2012).

Besides supporting the notion of a direct relationship between SCP/SCF and BOLD signals (He and Raichle, 2009; Raichle, 2011) and underlining that tDCS has extensive spatial and temporal effects on regional neuronal activity (Lang et al., 2005), our study extends previous metabolic neuroimaging studies by providing information on the direct effect of tDCS on SCF magnitudes across task-related brain regions. Our data underline that SCP/SCF carry information from these different cortical regions that is integrated over a rather slow time frame. Now that these cortical areas were identified, their specific contribution for integrating information during task performance should be investigated in future studies.

While assessment of electrical potentials, e.g. SCP, allows inferring the direction of cortical polarization (Elbert et al., 1981), i.e. increase in negativity or positivity that was attributed to strengthening or weakening of distant associative connections (Birbaumer et al., 1990), assessment of SCF does not allow such inference directly. This polarity ambiguity is a consequence of estimating the dipole source direction from the data, using a quadratic solution (in SAM). However, by taking previous EEG studies into account that provide information on the direction of cortical polarization during specific tasks, e.g. electric negativity over the vertex during preparation of a motor task (Birbaumer et al., 1990; Walter et al., 1964), the assumption is plausible that an increase in magnitude of SCF corresponds to an increase in cortical polarization assessed by EEG. Another possibility is to incorporate the cortical normal vector (extracted from a segmented anatomical MRI) as the orientation to be used in the beamformer solution in place of the quadratic solution used in SAM beamforming. In this case the beamformer will yield the absolute source polarity. Such approach, though, would require co-registration of the MEG and MRI frames of reference at an accuracy that exceeds present co-registration techniques (Hillebrand and Barnes, 2002). A more straightforward solution would be to co-register both MEG and EEG during tDCS, the latter combination recently shown to be feasible even during online brain-machine interface (BMI) control (Soekadar et al., 2014). Accurate topographical knowledge of cortical polarity shifts during anodal or cathodal tDCS and their direction would be important to understand the causal link between area- and hemisphere-specific polarity shifts and altered brain function or behavior (Kuo and Nitsche, 2015).

Birbaumer et al. (1990) proposed an integrative model to account for the regulation of selective attention and SCP based on the neuro-anatomical and network dynamics of the cortical basal-ganglia-thalamus-prefrontal cortex loop. According to this model, local increase of cortical excitation reflected in SCP's negativity at a particular brain area (Braitenberg and Schüz, 1991) is kept within physiological limits through this loop: increase of cortical excitation above certain thresholds, e.g. due to externally applied electric currents, causes compensatory inhibition supervised by prefrontal areas controlling selective opening and closing of the thalamic gates. While direct verification of this model has been difficult until now due to the non-availability of appropriate experimental methods, the here presented proof-of-principle study in which simultaneous tDCS was combined with whole-

Author Manuscript Author Manuscript Author Manuscript Author Manuscript

head MEG recordings suggests that specific hypotheses related to this or other integrative models can be tested in future.

While brain stimulation targeting specific brain areas was put forward as a tool to allow for causal neuroscience (Kuo and Nitsche, 2015), our data does not exclude such possibility, but suggests that a better understanding of local and particularly remote neurophysiological effects (e.g. as shown during cathodal M1 stimulation influencing SCF in the contralateral hemisphere's PPC) will be necessary. Such understanding may lead to better stimulation protocols and explain in part the large variability of stimulation effects reported in the literature.

Since this proof-of-principle study exemplified successful reconstruction of SCF in task-related brain areas during tDCS, reconstruction of activity in other frequency bands may allow to further elucidate other effects and cross-frequency relationships between field fluctuations and higher frequency brain oscillations (Monto et al., 2008; Vanhatalo et al., 2004), an issue important to improve understanding and interpretation of metabolic neuroimaging studies. While the influence of various factors such as gender, brain state, or genetic disposition (e.g. BDNF-Val66Met polymorphism) (Nieratschker et al., 2015) on tDCS-dependent modulation of SCF across various brain regions and motor performance was not investigated here, future studies that include these factors may further improve our understanding of inter-individual differences in responsiveness to electric brain stimulation.

While our results further support evidence for a shared neural substrate and direct relationship between SCF and BOLD signals most likely attributed to the synaptic activity of apical dendrites it cannot be excluded that also non-neuronal mechanisms, e.g. related to modulation of the blood–brain barrier or the neuro-vascular unit (Iadecola, 2004) contributed to the observed local and remote effects of tDCS.

Besides suggesting that TESANA can improve understanding of the relationship between neuromagnetic activity, brain function and behavior, it may also lead to the refinement of existing stimulation protocols by taking the temporal and spatial effects of electric brain stimulation into account. In this regard, extending the available spectrum of stimulation protocols used in concurrent tES/neuroimaging studies, particularly frequency-tuned transcranial alternating current stimulation (tACS) (Witkowski et al., 2016) or implementation of TESANA in closed-loop bidirectional brain-machine interface (BMI) systems (Liew et al., 2014; Soekadar et al., 2013b) may substantially advance the field.

Supplementary Material

Refer to Web version on PubMed Central for supplementary material.

Acknowledgments

The authors thank Christoph Braun and Birgit Teufel for their help in preparing the manuscript.

Finacial Disclosures

This work was supported by the Intramural Research Program (IRP) of the National Institute of Neurological Disorders and Stroke (NINDS) and National Institute of Mental Health (NIMH), Bethesda, Maryland, USA, the

Author Manuscript Author Manuscript Author Manuscript Author Manuscript

German Federal Ministry of Education and Research (BMBF, Föderzeichen 01GQ0831, 16SV5840), the Deutsche Forschungsgemeinschaft (DFG SO932-2), the European Union (FP7-ICT-2011-288551, Horizon 2020: AIDE 645322) and DAAD (Deutscher Akademischer Austauschdienst), *f*ortüne Program of the University of Tübingen's (No. 2216-0-0/F-No. 1331418) Medical Faculty, the Brain Products GmbH and Volkswagenstiftung. All authors reported no financial interests or potential conflicts of interest.

References

Antal A, Nitsche MA, Kincses TZ, Kruse W, Hoffmann KP, Paulus W. Facilitation of visuo-motor learning by transcranial direct current stimulation of the motor and extrastriate visual areas in humans. Eur. J. Neurosci. 2004; 19:2888–2892. [PubMed: 15147322]

Antal A, Polania R, Schmidt-Samoa C, Dechent P, Paulus W. Transcranial direct current stimulation over the primary motor cortex during fMRI. NeuroImage. 2011; 55:590–596. http://dx.doi.org/10.1016/j.neuroimage.2010.11.085. [PubMed: 21211569]

Birbaumer N, Elbert T, Canavan A, Rockstroh B. Slow potentials of the cerebral cortex and behavior. Physiol. Rev. 1990; 70:1–41. [PubMed: 2404287]

Boggio PS, Castro LO, Savagim EA, Braite R, Cruz VC, Rocha RR, et al. Enhancement of non-dominant hand motor function by anodal transcranial direct current stimulation. Neurosci. Lett. 2006; 404:232–236. [PubMed: 16808997]

Braitenberg, V., Schüz, A. Anatomy of the cortex—statistics and geometry. Springer-Verlag; Berlin: 1991. (Revised edition (1998) under the title: Cortex: statistics and geometry of neuronal connectivity)

Brunoni AR, Nitsche MA, Bolognini N, Bikson M, Wagner T, Merabet L, Edwards DJ, Valero-Cabre A, Rotenberg A, Pascual-Leone A, Ferrucci R, Priori A, Boggio PS, Fregni F. Clinical research with transcranial direct current stimulation (tDCS): challenges and future directions. Brain Stimul. 2012; 5:175–195. [PubMed: 22037126]

Creutzfeldt OD, Fromm GH, Kapp H. Influence of transcortical d-c currents on cortical neuronal activity. Exp. Neurol. 1962; 5:436–452. [PubMed: 13882165]

Dammers J, Ioannides AA. Neuromagnetic localization of CMV generators using incomplete and full-head biomagnetometer. NeuroImage. 2000; 3:167–178.

Dayan E, Censor N, Buch ER, Sandrini M, Cohen LG. Noninvasive brain stimulation: from physiology to network dynamics and back. Nat. Neurosci. 2013; 16:838–844. [PubMed: 23799477]

Elbert T, Lutzenberger W, Rockstroh B, Birbaumer N. The influence of low-level transcortical DC-currents on response speed in humans. Int. J. Neurosci. 1981; 14:101–114. [PubMed: 7263138]

Elbert T, Rockstroh B, Hampson S, Pantev C, Hoke M. The magnetic counterpart of the contingent negative variation. Electroencephalogr. Clin. Neurophysiol. 1994; 92:262–272. [PubMed: 7514995]

Ergenoglu T, Demiralp T, Beydagi H, Karamürsel S, Devrim M, Ermutlu N. Slow cortical potential shifts modulate P300 amplitude and topography in humans. Neurosci. Lett. 1998; 251:61–64. [PubMed: 9714465]

Feldman DE. Synaptic mechanisms for plasticity in neocortex. Annu. Rev. Neurosci. 2009; 32:33–55. [PubMed: 19400721]

Floden D, Stuss DT. Inhibitory control is slowed in patients with right superior medial frontal damage. J. Cogn. Neurosci. 2006; 18:1843–1849. [PubMed: 17069475]

Gartside IB. Mechanisms of sustained increases of firing rate of neurons in the rat cerebral cortex after polarization: role of protein synthesis. Nature. 1968; 220:383–384. [PubMed: 4300961]

Grubbs FE. Procedures for detecting outlying observations in samples. Technometrics. 1969; 11:1–21.

He BJ, Raichle ME. The fMRI signal, slow cortical potential and consciousness. Trends Cogn. Sci. 2009; 13:302–309. [PubMed: 19535283]

Helfrich RF, Knepper H, Nolte G, Strüber D, Rach S, Herrmann CS, Schneider TR, Engel AK. Selective modulation of interhemispheric functional connectivity by HD-tACS shapes perception. PLoS Biol. 2014; 12:e1002031. [PubMed: 25549264]

Author Manuscript Author Manuscript Author Manuscript Author Manuscript

Hendy AM, Kidgell DJ. Anodal-tDCS applied during unilateral strength training increases strength and corticospinal excitability in the untrained homologous muscle. Exp. Brain Res. 2014; 232:3243–3252. [PubMed: 24942703]

Hillebrand A, Barnes G. A quantitative assessment of the sensitivity of whole-head MEG to activity in the adult human cortex. NeuroImage. 2002; 16:1638–1650.

Hiltunen T, Kantola J, Abou Elseoud A, Lepola P, Suominen K, Starck T, Nikkinen J, Remes J, Tervonen O, Palva S, Kiviniemi V, Palva JM. Infra-slow EEG fluctuations are correlated with resting-state network dynamics in fMRI. J. Neurosci. 2014; 34:356–362. [PubMed: 24403137]

Hinds O, Thompson TW, Ghosh S, Yoo JJ, Whitfield-Gabrieli S, Triantafyllou C, Gabrieli JD. Roles of default-mode network and supplementary motor area in human vigilance performance: evidence from real-time fMRI. J. Neurophysiol. 2013; 109:1250–1258. [PubMed: 23236006]

Hummel F, Celnik P, Giraux P, Floel A, Wu WH, Gerloff C, Cohen LG. Effects of non-invasive cortical stimulation on skilled motor function in chronic stroke. Brain. 2005; 128:490–499. [PubMed: 15634731]

Iadecola C. Neurovascular regulation in the normal brain and in Alzheimer's disease. Nat. Rev. Neurosci. 2004; 5:347–360. [PubMed: 15100718]

Kayser C, Montemurro MA, Logothetis NK, Panzeri S. Spike-phase coding boosts and stabilizes information carried by spatial and temporal spike patterns. Neuron. 2009; 61:597–608. [PubMed: 19249279]

Keeser D, Meindl T, Bor J, Palm U, Pogarell O, Mulert C, Brunelin J, Möller HJ, Reiser M, Padberg F. Prefrontal transcranial direct current stimulation changes connectivity of resting-state networks during fMRI. J. Neurosci. 2011; 31:15284–15293. [PubMed: 22031874]

Konen CS, Mruczek RE, Montoya JL, Kastner S. Functional organization of human posterior parietal cortex: grasping- and reaching-related activations relative to topographically organized cortex. J. Neurophysiol. 2013; 109:2897–2908. [PubMed: 23515795]

Kuo MF, Nitsche MA. Exploring prefrontal cortex functions in healthy humans by transcranial electrical stimulation. Neurosci. Bull. 2015; 31:198–206. [PubMed: 25680572]

Kuo MF, Paulus W, Nitsche MA. Therapeutic effects of non-invasive brain stimulation with direct currents (tDCS) in neuropsychiatric diseases. NeuroImage. 2014; 85:948–960. [PubMed: 23747962]

Lang N, Siebner HR, Ward NS, Lee L, Nitsche MA, Paulus W, et al. How does transcranial DC stimulation of the primary motor cortex alter regional neuronal activity in the human brain? Eur. J. Neurosci. 2005; 22:495–504. [PubMed: 16045502]

Liew SL, Santarnecchi E, Buch ER, Cohen LG. Non-invasive brain stimulation in neurorehabilitation: local and distant effects for motor recovery. Front. Hum. Neurosci. 2014; 8:378. [PubMed: 25018714]

Monti A, Ferrucci R, Fumagalli M, Mameli F, Cogiamanian F, Ardolino G, Priori A. Transcranial direct current stimulation (tDCS) and language. J. Neurol. Neurosurg. Psychiatry. 2013; 84:832–842. [PubMed: 23138766]

Monto S, Palva S, Voipio J, Palva JM. Very slow EEG fluctuations predict the dynamics of stimulus detection and oscillation amplitudes in humans. J. Neurosci. 2008; 28:8268–8272. [PubMed: 18701689]

Nieratschker V, Kiefer C, Giel K, Krüger R, Plewnia C. The COMT Val/Met polymorphism modulates effects of tDCS on response inhibition. Brain Stimul. 2015; 8:283–288. [PubMed: 25496958]

Nitsche MA, Paulus W. Excitability changes induced in the human motor cortex by weak transcranial direct current stimulation. J. Physiol. 2000; 527:633–639. [PubMed: 10990547]

Nitsche MA, Koschack J, Pohlers H, Hullemann S, Paulus W, Happe S. Effects of frontal transcranial direct current stimulation on emotional state and processing in healthy humans. Front. Psychiatry. 2012; 3:58. [PubMed: 22723786]

Oostenveld R, Fries P, Maris E, Schoffelen J-M. FieldTrip: open source software for advanced analysis of MEG, EEG, and invasive electrophysiological data. Comput. Intell. Neurosci. 2011:156869. [PubMed: 21253357]

Paulus W. Outlasting excitability shifts induced by direct current stimulation of the human brain. Suppl. Clin. Neurophysiol. 2004w; 57:708–714. in review. [PubMed: 16106673]

Author Manuscript Author Manuscript Author Manuscript Author Manuscript

Pellicciari MC, Brignani D, Miniussi C. Excitability modulation of the motor system induced by transcranial direct current stimulation: a multimodal approach. NeuroImage. 2013; 83:569–580. [PubMed: 23845429]

Pena-Gomez C, Sala-Lonch R, Junqué C, Clemente IC, Vidal D, Bargalló N, et al. Modulation of large-scale brain networks by transcranial direct current stimulation evidenced by resting-state functional MRI. Brain Stimul. 2012; 5:252–263. [PubMed: 21962981]

Purpura DP, Mcmurtry JG. Intracellular activities and evoked potential changes during polarization of motor cortex. J. Neurophysiol. 1965; 28:166–185. [PubMed: 14244793]

Raichle ME. The restless brain. Brain Connect. 2011; 1:3–12. [PubMed: 22432951]

Rebert CS. Slow potential correlates of neuronal population responses in the cat's lateral geniculate nucleus. Electroencephalogr. Clin. Neurophysiol. 1973; 35:511–515. [PubMed: 4126457]

Robinson, E., Vrba, J. Functional neuroimaging by synthetic aperture magnetometry (SAM).. In: Yoshimoto, T.Kuriki, S.Karibe, H., Nakasato, N., editors. Recent Adv. Biomagn. Tohoku University Press; Sendai: 1999. p. 302-305.

Rockstroh, B., Elbert, T., Canavan, A., Lutzenberger, W., Birbaumer, N. Slow Cortical Potentials Behav. Urban Schwarzenberg; Munich: 1989. Slow potentials of the brain..

Rösler F, Heil M, Röder B. Slow negative brain potentials as reflections of specific modular resources of cognition. Biol. Psychol. 1997; 45:109–141. [PubMed: 9083647]

Rossini P, Barker A, Berardelli A, Caramia M, Caruso G, Cracco R, et al. Noninvasive electrical and magnetic stimulation of the brain, spinal cord and roots: basic principles and procedures for routine clinical application. Report of an IFCN committee. Electroencephalogr. Clin. Neurophysiol. 1994; 91:79–92. [PubMed: 7519144]

Santarnecchi E, Polizzotto NR, Godone M, Giovannelli F, Feurra M, Matzen L, Rossi A, Rossi S. Frequency-dependent enhancement of fluid intelligence induced by transcranial oscillatory potentials. Curr. Biol. 2013; 23:1449–1453. [PubMed: 23891115]

Soekadar SR, Witkowski M, García Cossio E, Birbaumer N, Robinson SE, Cohen LG. In vivo assessment of human brain oscillations during application of transcranial electric currents. Nat. Commun. 2013a; 4:2032. [PubMed: 23787780]

Soekadar SR, Witkowski M, Robinson SE, Birbaumer N. Combining electric brain stimulation and source-based brain-machine interface (BMI) training in neurorehabilitation of chronic stroke. J. Neurol. Sci. 2013b:e333–e542.

Soekadar SR, Witkowski M, García Cossio E, Birbaumer N, Cohen LG. Learned EEG-based brain self-regulation of motor-related oscillations during application of transcranial electric brain stimulation: feasibility and limitations. Front. Behav. Neurosci. 2014; 8:93. [PubMed: 24672456]

Soekadar SR, Witkowski M, Birbaumer N, Cohen LG. Enhancing hebbian learning to control oscillatory activity. Cereb. Cortex. 2015; 25:2409–2415. [PubMed: 24626608]

Stagg CJ, O'Shea J, Kincses ZT, Woolrich M, Matthews PM, Johansen-Berg H. Modulation of movement-associated cortical activation by transcranial direct current stimulation. Eur. J. Neurosci. 2009; 30:1412–1423. [PubMed: 19788568]

Talati A, Hirsch J. Functional specialization within the medial frontal gyrus for perceptual go/no-go decisions based on “what,” “when,” and “where” related information: an fMRI study. J. Cogn. Neurosci. 2005; 17:981–993. [PubMed: 16102231]

Vanhatalo S, Palva JM, Holmes MD, Miller JW, Voipio J, Kaila K. Infraslow oscillations modulate excitability and interictal epileptic activity in the human cortex during sleep. Proc. Natl. Acad. Sci. U. S. A. 2004; 101:5053–5057. [PubMed: 15044698]

Voss U, Holzmann R, Hobson A, Paulus W, Koppehele-Gossel J, Klimke A, Nitsche MA. Induction of self awareness in dreams through frontal low current stimulation of gamma activity. Nat. Neurosci. 2014; 17:810–812. [PubMed: 24816141]

Walter WG, Cooper R, Aldridge VJ, McCallum WC, Winter AL. Contingent negative variation: an electrical sign of sensori-motor association and expectancy in the human brain. Nature. 1964; 203:380–384. [PubMed: 14197376]

Wang XJ. Neurophysiological and computational principles of cortical rhythms in cognition. Physiol. Rev. 2010; 90:1195–1268. [PubMed: 20664082]

Author Manuscript Author Manuscript Author Manuscript Author Manuscript

Witkowski M, Garcia-Cossio E, Chander B, Braun C, Birbaumer N, Robinson SE, Soekadar SR. Mapping entrained brain oscillations during transcranial alternating current stimulation. NeuroImage. 2016; 104:89–98.

Author Manuscript Author Manuscript Author Manuscript Author Manuscript

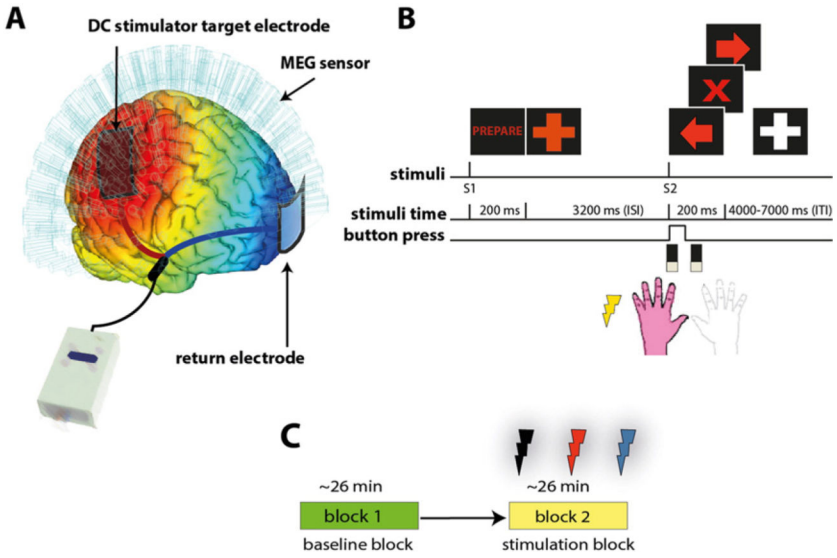

Fig. 1.

Experimental setup and design. (A) Transcranial direct current stimulation (tDCS) inside the whole-head MEG helmet was applied using a bipolar montage. For anodal stimulation, the target electrode (indicated in red) was placed above the right primary motor cortex (M1) while the return electrode (indicated in blue) was placed over the left supraorbita. For cathodal stimulation, the polarity of the electric current was inverted. (B) Illustration of the S1–S2 paradigm. The word "PREPARE" was visually presented as *warning* stimulus (S1) followed by a red cross. Thereafter, one of three different symbols (the *imperative* stimulus S2) was displayed in a random order (red arrow to the right, red arrow to the left or red cross). Depending on the symbol, participants had to press either a left, right or no button depending on the displayed symbol. (C) Participants attended three experimental sessions and received either anodal, cathodal or sham tDCS in a randomized order. Each experimental session consisted of two blocks: a baseline block (in absence of stimulation) and a stimulation block (anodal, cathodal, sham).

Author Manuscript Author Manuscript Author Manuscript Author Manuscript

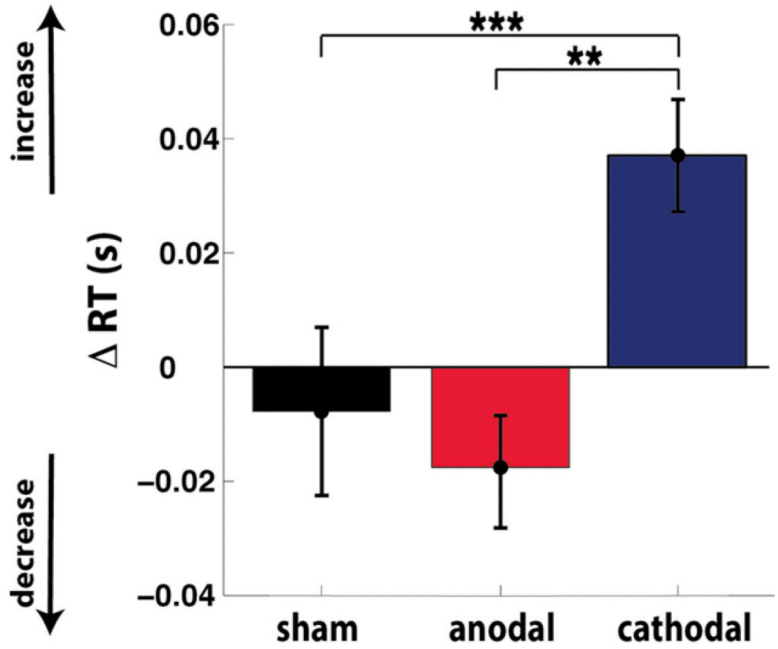

Fig. 2.

Impact of sham (black), anodal (red) and cathodal (blue) tDCS on reaction time (RT) (mean ± SE). **p ≤ 0.01, ***p ≤ 0.001.

Author Manuscript Author Manuscript Author Manuscript Author Manuscript

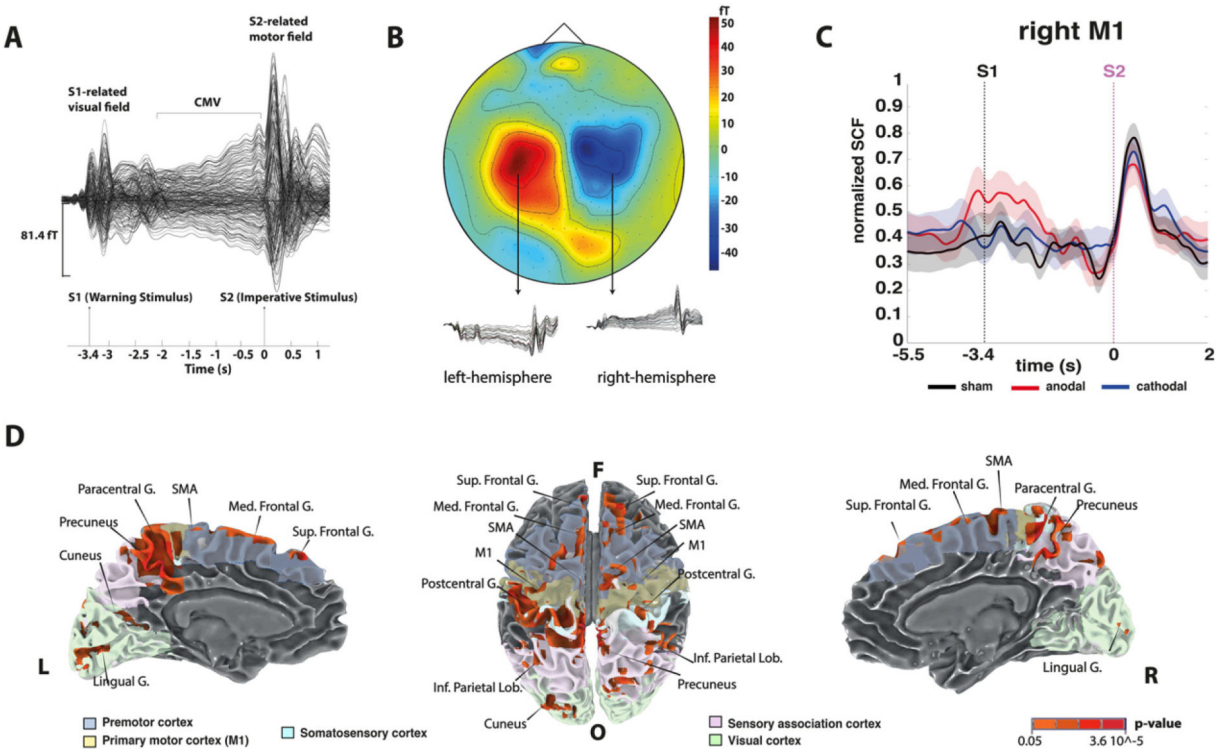

Fig. 3.

The contingent magnetic variation (CMV) grand average across participants with its typical S1–S2 waveform as described by Elbert et al. (1994) is shown in (A). (B) Topographical distribution of the CMV averaged over the time interval from −1 s prior to S2 till the onset of S2. The CMV grand average of the activity recorded at MEG sensors with maximum slow cortical field (SCF) magnitude in the right (blue) and left (red) sensor array are plotted in the lower part of the panel. (C) Waveform of source-reconstructed slow cortical fields (SCF) in the right primary motor cortex (M1) during and in absence of tDCS. (D) Localization of SCF related to left button presses matched brain regions described in previous metabolic neuroimaging studies (Lang et al., 2005; Stagg et al., 2009), and included pre-motor, motor and posterior parietal cortical (PPC) areas ($p \leq 0.05$ corrected, cluster size: 25 voxels).

Author Manuscript Author Manuscript Author Manuscript Author Manuscript

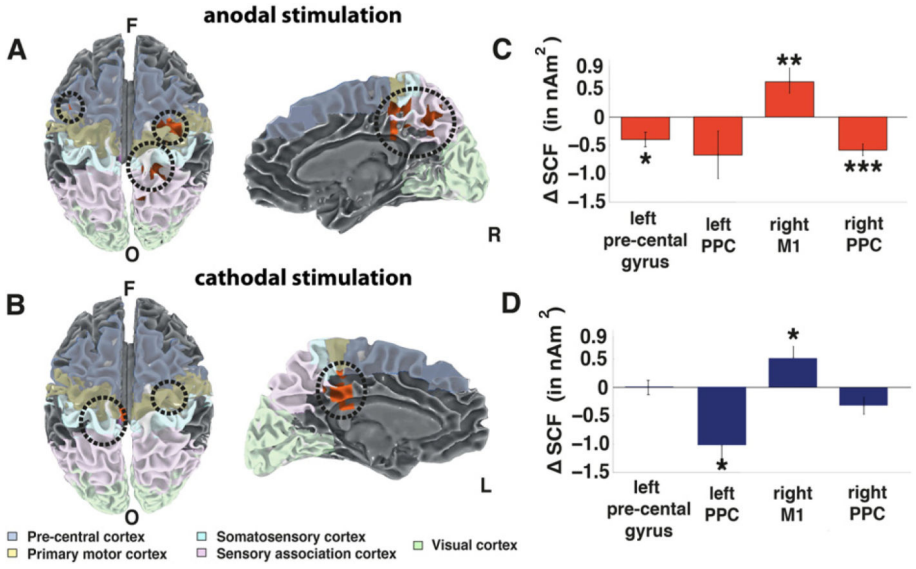

Fig. 4.

Task-related brain regions (marked by dotted black circles) in which anodal tDCS had an impact on SCF were localized in the right primary motor cortex (M1, primary stimulation site), right posterior parietal cortex (PPC) and left pre-motor areas (A–C). Similarly, SCF of the right M1 became also affected by cathodal tDCS while having its main impact on SCF of the contralateral, left PPC on the non-stimulated hemisphere. *Indicates a significant difference between anodal or cathodal stimulation in comparison to sham stimulation. *$p \leq 0.05$, **$p \leq 0.01$, ***$p \leq 0.001$ ($p \leq 0.05$ corrected, cluster size 13), error bars indicate the standard error (SE).